ARTICLE OPEN

Nutrient-regulated dynamics of chondroprogenitors in the postnatal murine growth plate

Takeshi Oichi[1,2,3]✉, Joe Kodama[1], Kimberly Wilson[1], Hongying Tian[1], Yuka Imamura Kawasawa[4], Yu Usami[5], Yasushi Oshima[2], Taku Saito[2], Sakae Tanaka[2], Masahiro Iwamoto[1], Satoru Otsuru[1] and Motomi Enomoto-Iwamoto[1]✉

Longitudinal bone growth relies on endochondral ossification in the cartilaginous growth plate, where chondrocytes accumulate and synthesize the matrix scaffold that is replaced by bone. The chondroprogenitors in the resting zone maintain the continuous turnover of chondrocytes in the growth plate. Malnutrition is a leading cause of growth retardation in children; however, after recovery from nutrient deprivation, bone growth is accelerated beyond the normal rate, a phenomenon termed catch-up growth. Although nutritional status is a known regulator of long bone growth, it is largely unknown whether and how chondroprogenitor cells respond to deviations in nutrient availability. Here, using fate-mapping analysis in *Axin2Cre*^{ERT2} mice, we showed that dietary restriction increased the number of Axin2^{+} chondroprogenitors in the resting zone and simultaneously inhibited their differentiation. Once nutrient deficiency was resolved, the accumulated chondroprogenitor cells immediately restarted differentiation and formed chondrocyte columns, contributing to accelerated growth. Furthermore, we showed that nutrient deprivation reduced the level of phosphorylated Akt in the resting zone and that exogenous IGF-1 restored the phosphorylated Akt level and stimulated differentiation of the pooled chondroprogenitors, decreasing their numbers. Our study of *Axin2Cre*^{ERT2} revealed that nutrient availability regulates the balance between accumulation and differentiation of chondroprogenitors in the growth plate and further demonstrated that IGF-1 partially mediates this regulation by promoting the committed differentiation of chondroprogenitor cells.

Bone Research (2023)11:20 ; https://doi.org/10.1038/s41413-023-00258-9

INTRODUCTION

Long bone growth is promoted by endochondral ossification that occurs at growth plates, which are cartilaginous tissues at the ends of long bones and vertebral bodies.[1] The growth plate comprises three layers: the resting, proliferative, and hypertrophic zones. The resting zone contains round, undifferentiated chondrocytes (hereafter "chondroprogenitors") that rarely divide and are precursors to proliferative chondrocytes.[2,3] Recent lineage-tracing studies have identified chondroprogenitors in the resting zone that contribute continually to long bone growth via the acquisition of stem-cell characteristics after the formation of the secondary ossification center (SOC).[4,5] A genome-wide association study of human height revealed that the specificity of gene expression in the resting chondrocytes in newborn mice is significantly associated with height GWAS *p* values, stressing the important role of these cell populations in determining human skeletal growth.[6]

Malnutrition is considered a leading cause of growth retardation in children.[7,8] When transient nutritional impairment is resolved, the long bone growth rate often accelerates beyond the normal rate; this phenomenon is termed catch-up growth.[9] A common hypothesis to explain catch-up growth is that growth-inhibiting conditions decrease the proliferation of chondroprogenitors, preserving their proliferative potential until the growth-inhibiting conditions are resolved, at which point the preserved proliferative capacity accelerates growth.[10] Although this hypothesis suggests that chondroprogenitors play an important role in this phenomenon, the effect of nutritional availability on their function is poorly understood. One reason for the limited research on this topic is the lack of appropriate tools to mark and visualize chondroprogenitors at appropriate times.

Wnt proteins participate in the maintenance of stem cells in many adult mammalian tissues.[11] Wnt signaling is mediated by a pathway that activates transcription factors via the intracellular protein β-catenin. Axin2, a universal transcriptional target of β-catenin-dependent Wnt signaling, provides a reliable readout of cell responses to Wnt.[11,12] Genetic lineage tracing of the cells marked by reporter protein expression in *Axin2Cre*^{ERT2} mice successfully identified stem cells in several adult mammalian tissues.[13–16] We used this lineage tracing approach to identify a unique population of Axin2^{+} chondroprogenitor cells that reside in the resting zone of the growth plate after SOC formation. In this study, we investigated the nutrient-regulated dynamics of these chondroprogenitors and their regulatory mechanism using fate mapping analysis with a mouse nutrient-induced catch-up growth model.

[1]Department of Orthopedics, School of Medicine, University of Maryland, Baltimore, MD 21201, USA; [2]Sensory & Motor System Medicine, Faculty of Medicine, The University of Tokyo, Bunkyo-ku, Tokyo 1138655, Japan; [3]Department of Orthopedics, Teikyo University School of Medicine, Tokyo 1738608, Japan; [4]Department of Biochemistry and Molecular Biology, Pennsylvania State University College of Medicine, Hershey, PA 17033, USA and [5]Department of Oral Pathology, Osaka University Graduate School of Dentistry, Suita, Osaka 5650871, Japan
Correspondence: Takeshi Oichi (oichi-tky@umin.ac.jp) or Motomi Enomoto-Iwamoto (motomi.iwamoto@som.umaryland.edu)

Received: 3 April 2022 Revised: 3 March 2023 Accepted: 9 March 2023
Published online: 21 April 2023

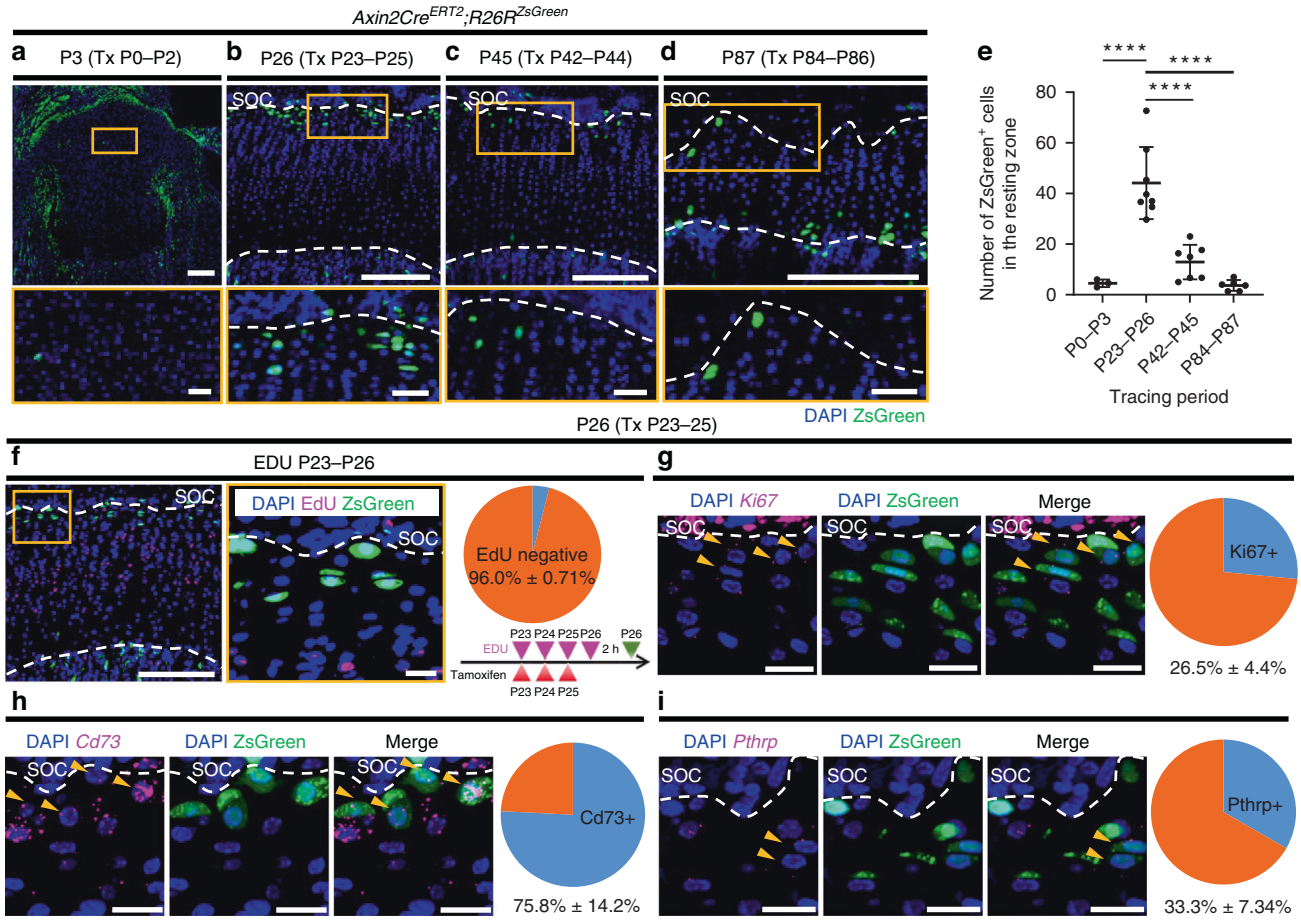

Fig. 1 Identification and characterization of Axin2$^+$ cells in the resting zone after secondary ossification center formation. **a**–**d** Axin2$^+$ cells in the proximal tibial growth plate in *Axin2Cre^{ERT2};R26R^{ZsGreen}* mice. Axin2$^+$ cells were labeled one day after three consecutive daily injections of tamoxifen (120 μg·g^{-1} body weight) from P0 ($n = 3$) (**a**), P23 ($n = 8$) (**b**), P42 ($n = 7$) (**c**), and P84 ($n = 6$) (**d**). Bottom panels show magnified views of the resting zone of the growth plate. **e** Quantification of ZsGreen$^+$ cells in the resting zone across different time points reported above in (**a**–**d**). Adjusted ****$P =< 0.000\,1$. **f**–**i** Characterization of Axin2$^+$ cells in the resting zone of the proximal tibial growth plate in *Axin2Cre^{ERT2};R26R^{ZsGreen}* mice one day after three consecutive daily tamoxifen injections from P23. **f** Representative images of EdU labeling and Axin2$^+$ cells and the percentage of EdU-negative cells among Axin2$^+$ cells ($n = 3$). EdU (30 μg/g body weight) was injected daily from P23 to P26, and mice were euthanized 2 h after the last administration of EdU. **g** Representative images of in situ hybridization of *Ki67* and Axin2$^+$ cells and the percentage of Ki67+ cells among Axin2$^+$ cells ($n = 3$). Arrow heads, Axin2$^+$ cells expressing *Ki67*. **h** Representative images of in situ hybridization of *Cd73* and Axin2$^+$ cells and the percentage of *Cd73*$^+$ cells among Axin2$^+$ cells ($n = 3$). Arrow heads, Axin2$^+$ cells expressing *Cd73*. i Representative images of in situ hybridization of *Pthrp* and Axin2$^+$ cells and the percentage of *Pthrp*$^+$ cells among Axin2$^+$ cells ($n = 3$). Arrow heads, Axin2$^+$ cells expressing *Pthrp*. Tx tamoxifen, SOC secondary ossification center. The white dashed lines demarcate the growth plate from the surrounding tissues. Scale bars: 200 μm (**a**–**d** [upper panels], **f** [left]), 40 μm (**a**–**d** [bottom panels]), 20 μm (**f** [right], **g**–**i**). All data are presented as the mean ± SD. Statistical significance was determined by one-way analysis of variance and Tukey's multiple comparison test

RESULTS

Identification of Axin2$^+$ cells in the resting zone of the growth plate after SOC formation

We first investigated whether Axin2-expressing cells contain chondroprogenitors in the resting zone of the growth plate because the *Axin2* gene has been successfully used to identify tissue-specific stem cells in other tissues.[13–16] Administration of tamoxifen for three consecutive days induced Cre-mediated expression of the R26RZsGreen reporter, showing that Axin2$^+$ cells were rarely present in the resting zone of the neonatal growth plate (Fig. 1a and e). However, these cells appeared in the resting zone after SOC formation (Fig. 1b, proximal tibia and Fig. S1, distal femur), which is consistent with a previous study,[17] and the number of these Axin2$^+$ cells in the resting zone decreased when tamoxifen induction was performed at older ages (Fig. 1c–e). The highly specific localization of Axin2$^+$ cells in the growth plate was observed at all ages after SOC formation, suggesting that chondroprogenitor cells in the resting zone were labeled.

We focused on Axin2$^+$ cells in the resting zone at P23 because the SOC is fully developed by this time and growth plate activity is high at this time.[5] To characterize these Axin2$^+$ cells, we isolated chondrocytes from the growth plate of *Axin2Cre^{ERT2};R26R^{ZsGreen}* mice at P26 after tamoxifen injections at P23-P25 and assessed them for skeletal stem cell markers as reported previously (Fig. S2a).[18] Axin2$^+$ cells were distributed into various types of stem cell populations, including 'multipotent progenitors' and 'stromal progenitors' (Fig. S2b), and 41.8% of the total Axin2$^+$ cells were fractionated into the 'multipotent progenitor' population, characterized as CD45$^-$TER119$^-$Tie2$^-$AlphaV$^+$Thy$^-$6C3$^-$CD105$^-$CD200$^+$ cells (Fig. S2c). To test whether Axin2$^+$ cells and their descendants have stem cell-like properties in cultured conditions, we isolated the cells from the growth plate of *Axin2Cre^{ERT2};R26R^{ZsGreen}* mice at P37 after tamoxifen injections at P23-P25 and expanded them by serial passaging. At Passage 6, the cells stopped proliferating; the population doubling level when they ceased proliferation was approximately 13.0. The percentage of ZsGreen-positive cells was

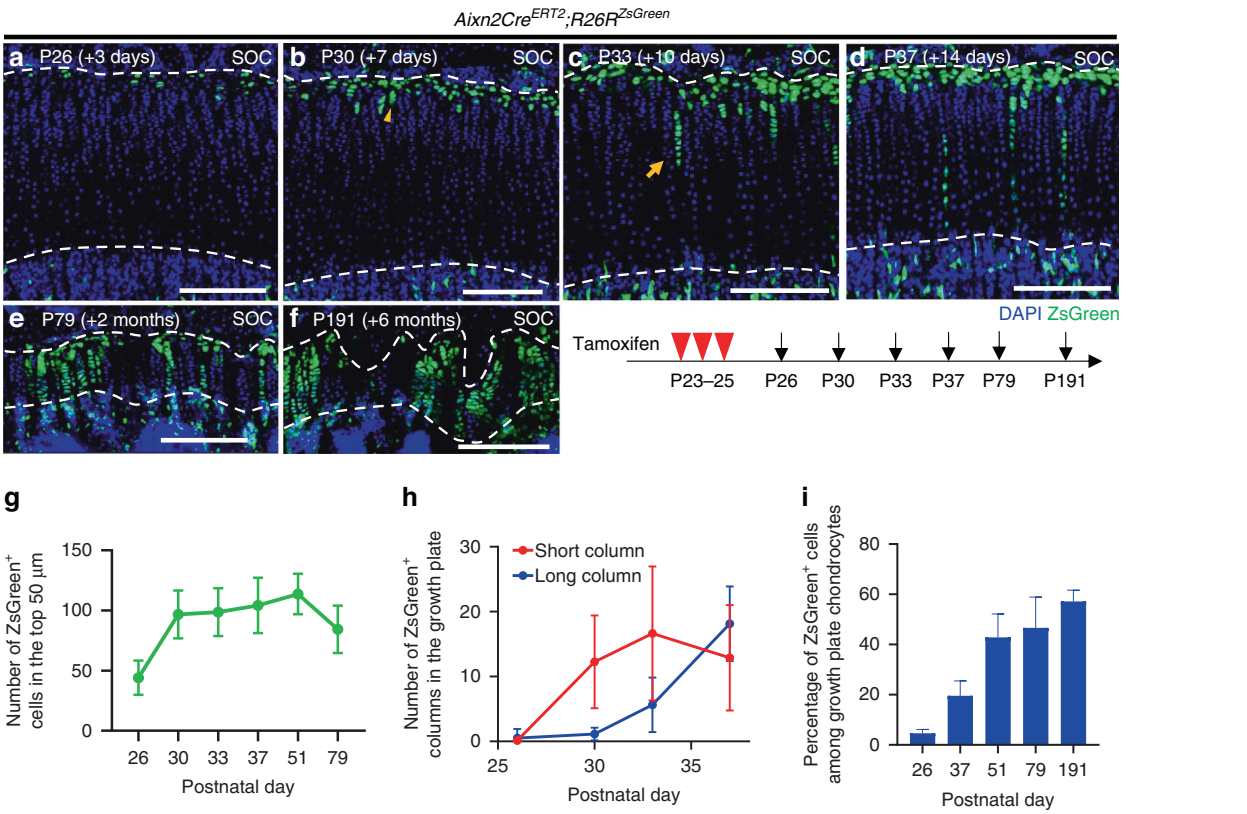

Fig. 2 Axin2$^+$ cells include a subset of chondroprogenitors in the growth plate. **a**–**f** Fate-mapping analysis of Axin2$^+$ cells in the proximal tibial growth plate in *Axin2Cre^{ERT2};R26R^{ZsGreen}* mice (pulsed on P23–25 and traced for several days). Representative images showing descendants of initially labeled Axin2$^+$ cells at 3 ($n = 8$) (**a**), 7 ($n = 8$) (**b**), 10 ($n = 8$) (**c**) and 14 ($n = 8$) (**d**) days and at 2 ($n = 7$) (**e**) and 6 ($n = 6$) (**f**) months after tamoxifen injection. Arrowhead, short column (≤9 cells) (**b**); arrows, long column (≥10 cells) (**c**). **g**–**i** Quantification of ZsGreen$^+$ cells in the top 50 μm (green line) (**g**), ZsGreen$^+$ columns in the growth plate, short columns (≤9 cells, red line) and long columns (≥10 cells, blue line) (**h**), and percentage of ZsGreen$^+$ cells among growth plate chondrocytes (blue bars) (**i**). P26–P51 ($n = 8$), P79 ($n = 7$), and P191 ($n = 6$). SOC secondary ossification center. The white dashed lines demarcate the growth plate from the surrounding tissues. Scale bars: 200 μm (**a**–**f**). All data are presented as the mean ± SD

32% ± 7.5% at Passage 3 and 42% ± 8.2% at Passage 5. At Passage 3, the ZsGreen-positive cells were sorted and cultured under chondrogenic, osteogenic and adipogenic differentiation conditions. The ZsGreen-positive cells showed accumulation of sulfated proteoglycan, calcification and oil droplets under chondrogenic, osteogenic and adipogenic differentiation conditions, respectively (Fig. S2d). These results suggest that Axin2$^+$ cells have chondrogenic, osteogenic and adipogenic differentiation abilities, but their expansion ability is limited.

To examine the proliferative activity of these Axin2$^+$ cells, we performed an EdU label-exclusive assay and in situ hybridization of *Mki67* (*Ki67*). Most Axin2$^+$ cells excluded EdU (Fig. 1f, EdU$^-$; 96.0% ± 0.71% of ZsGreen$^+$ cells, $n = 3$ mice), and approximately 70% of Axin2$^+$ cells did not express *Ki67* (Fig. 1g, *Ki67*$^+$; 26.5% ± 4.4% of ZsGreen$^+$ cells, $n = 3$ mice), suggesting that Axin2$^+$ cells represent slow-cycling cells. We then examined the expression of *Nt5e* (*Cd73*) and *Pthlh* (*Pthrp*), which are previously reported stem cell markers of resting chondrocytes.[4,5] A large population of Axin2$^+$ cells expressed *Cd73* (Fig. 1h, *Cd73*$^+$;75.8% ± 14.2% of ZsGreen$^+$ cells, $n = 3$ mice), and approximately one-third of Axin2$^+$ cells expressed *Pthrp* (Fig. 1i, *Pthrp*$^+$; 33.3% ± 7.34% of ZsGreen$^+$ cells, $n = 3$ mice). *Foxa2*-expressing cells have been identified to be present close to the SOC in the resting zone and to contribute to growth plate renewal.[19] At P26, *Foxa2* transcripts were sparsely expressed in the resting and proliferative chondrocytes but were abundantly expressed in the hypertrophic chondrocytes (Fig. S3a). Cells immunoreactive to the anti-Foxa2 antibody were detected at the border of the SOC, with some of the cells being ZsGreen positive (Fig. S3b, arrowhead). These data suggest that the identified Axin2$^+$ cells included a subset of previously reported chondroprogenitors.

Self-renewal and differentiation of Axin2$^+$ cells

To determine the self-renewal ability of Axin2$^+$ cells and their contribution to growth plate maintenance, we performed a series of cell tracing analyses in *Axin2Cre^{ERT2};R26R^{ZsGreen}* mice. After remaining in the resting zone (P26, Fig. 2a), the descendants of the initially labeled Axin2$^+$ cells (hereafter, *Axin2-creER*$^+$ cells) first formed short columns (composed of <10 cells) after 7 days of chase (P30, Fig. 2b, arrowhead) and subsequently formed long columns (composed of ≥10 cells) after 10 days of chase (P33, Fig. 2c, arrow). After two weeks of chase, *Axin2-creER*$^+$ cells had constituted the columns encompassing the resting to hypertrophic zones (P37, Fig. 2d, proximal tibia and Fig. S1, distal femur). The number of ZsGreen$^+$ cells in the top 50 μm zone increased during the first month of chase and decreased thereafter (Fig. 2a–e, g). The number of short ZsGreen$^+$ columns increased from P23 to P30 and then plateaued, whereas long ZsGreen$^+$ columns appeared at P33, and their number increased over time (Fig. 2h). *Axin2-creER*$^+$ cells continued to accumulate over a long chase period (Fig. 2i) and formed chondrocyte columns in the growth plate after at least six months of tracing (Fig. 2f). We analyzed the data of lineage tracing experiments in male and female *Axin2Cre^{ERT2};R26R^{ZsGreen}* mice because there were no significant sex differences in the number of ZsGreen$^+$ cells in the top 50 μm zone, the number of short/long ZsGreen$^+$ columns,

and the percentage of ZsGreen$^+$ cells among the growth plate chondrocytes (Fig. S4a–d).

To investigate whether ZsGreen$^+$ chondrocyte columns existed in the same clone, we analyzed *Axin2Cre^{ERT2};R26R^{Confetti}* mice. The administration of tamoxifen for five consecutive days from P23 marked Axin2$^+$ cells in the resting zone (Fig. S5a, orange arrowheads), enabling us to perform clonal analyses. After three months of chase, some *Axin2-creER$^+$* cells formed chondrocyte columns labeled in the same color (Fig. S5b, orange arrow and Fig. S5d, magenta, 23.3% ± 6.35%), indicating that a single Axin2$^+$ resting chondrocyte can give rise to the entire chondrocyte column. In contrast, some *Axin2-creER$^+$* cells remained in singlet (Fig. S5c, white arrow and Fig. S5d, black, 38.9% ± 6.89%) or doublet form (Fig. S5c, white arrowhead and Fig. S5d, blue, 34.8% ± 7.14%) in the resting zone, indicating that some Axin2$^+$ cells can be dormant or very slow-proliferating resting chondrocytes. Together, these findings showed that Axin2$^+$ cells included a subset of chondroprogenitors with self-renewal capability to continually form growth plate chondrocytes during the bone growth period.

We next examined whether Axin2$^+$ cells at different developmental stages had the capacity to form chondrocyte columns. The Axin2$^+$ cells at both P45 and P87 were found in the resting zone (Fig. 1b–d and Fig. S6a–c) in a similar distribution to that observed at P26 (Fig. 1b and Fig. S6a). Interestingly, Axin2$^+$ cells were also observed in the hypertrophic zone at P87 (Fig. S6c), suggesting that Wnt/β-catenin signaling was highly activated in the hypertrophic zone at this time. After one month of chase analysis, Axin2$^+$ cells initially labeled at both P45 and P87 had produced long chondrocyte columns (Fig. S6e, arrows, and Fig. S6f, arrow). The percentage of *Axin2-CreER$^+$* cells among growth plate chondrocytes after 28 days of chase decreased with time (Fig. S6d–g). These data suggested that Axin2$^+$ cells in the resting zone retained the ability to generate chondrocyte columns over time, although their contribution to growth plate chondrocytes declined with age.

Establishment of the mouse catch-up growth model

To investigate changes in the distributions of *Axin2-CreER$^+$* cells during malnutrition and subsequent catch-up growth, we first developed a mouse catch-up growth model. The mice were fed ad libitum from the start (control group) or subjected to a 50% dietary restriction (DR) for seven days from P27 before ad libitum feeding (catch-up group) (Fig. S7a). During the seven-day DR period, the male and female catch-up group mice gained less weight than the control group mice (male, $P = 0.002\,3$, and female, $P = 0.012\,0$; Fig. S7b, c). During the first five days after DR, the male and female mice in the catch-up group gained weight more rapidly than the control mice (male, $P = 0.000\,5$, and female, $P = 0.025\,9$; Fig. S7b, c), and there were no significant differences in body weight at the end of the experiment for both males and females (Fig. S7b, c).

The tibial length of male mice in the catch-up group was 0.64 mm less than that of the control animals at P34 ($P = 0.018\,6$; Fig. S7d). Progressive catch-up growth occurred ($P = 0.000\,8$), reducing this deficit to 0.02 mm (not significant) at P62 (Fig. S7d). Similarly, the tibial length of the female mice in the catch-up group was 0.75 mm less than that of the control animals at P34 ($P = 0.016\,3$; Fig. S7e), and progressive catch-up growth occurred ($P = 0.015$), reducing this deficit to 0.10 mm (not significant) at P62 (Fig. S7e). Proximal tibial growth rates, measured by alizarin labeling, were significantly reduced by seven-day DR compared with those of the control groups for both males and females ($P < 0.000\,1$ and $P = 0.003\,9$, respectively; Fig. S7f, g). Marked increases were observed in the growth rate of the catch-up group mice between P34 and P41 in both males and females ($P = 0.009\,5$ and $P = 0.016\,6$, respectively; Fig. S7f, g). The growth rate in the catch-up group then gradually decreased but remained greater than that of the control group, at least until P48, in both males and females (Fig. S7f, g). The *Axin2Cre^{ERT2};R26R^{ZsGreen}* mice showed a similar reduction in the growth rate during the seven-day DR compared to that of the control group ($P < 0.000\,1$) and an increase in the growth rate after refeeding ($P = 0.011\,9$) (Fig. S8a).

Histomorphometric analysis revealed that DR reduced the lengths of the total growth plate and hypertrophic zone (Fig. S7h). However, DR increased the ratio of the length of the resting zone to that of the total growth plate but did not change the ratio of the length of other zones to that of the total growth plate (Fig. S7h). During catch-up growth, the growth plate length was significantly increased compared to the ad libitum control after stopping DR (Fig. S7i). The ratio of the hypertrophic zone to the total growth plate length was not significantly different between these two groups at any time point (Fig. S7i). The EdU incorporation rate in the growth plate was markedly reduced by DR and was recovered 2 days after stopping DR (Fig. S7j).

DR enhances self-replication of resting chondrocytes while inhibiting their differentiation

The behavior of chondroprogenitors during DR and following catch-up growth was investigated by applying lineage tracing analysis in *Axin2Cre^{ERT2};R26R^{ZsGreen}* mice to the mouse catch-up growth model. First, we examined the effect of seven days of DR on the distribution of *Axin2-CreER$^+$* cells in the proximal tibial growth plate. After tamoxifen administration for three consecutive days from P23, the mice were fed ad libitum (control group) or subjected to seven days of DR (DR group) (Fig. 3a). After 11 days of tracing (P34), *Axin2-CreER$^+$* cells had formed fewer chondrocyte columns in the DR group than in the control group (Fig. 3b–d). In support of this finding, histological analysis revealed that the growth plates of the DR mice showed reduced chondrocyte column density compared with those of the control mice (Fig. 3i–k). DR led to a 30% increase in the number of ZsGreen$^+$ cells in the top 50 μm zone compared to that in the control group (Fig. 3b, c, e). To independently confirm this observation, we performed in situ hybridization of *Clusterin* (*Clu*), whose expression has been detected in the resting zone as well as in the articular cartilage,[20] to quantify the number of resting chondrocytes. We chose *Clu* as a marker for resting chondrocytes because *Clu* expression was more abundant and more selective for resting chondrocytes than previously reported markers for resting chondrocytes, including *Cd73*, *Pthlp* and *Foxa2* (Fig. S9a, b). The number of *Clu$^+$* resting chondrocytes was 56% higher in the DR mice than in the control mice (Fig. 3f–h).

The observation of an increased number of resting chondrocytes with inhibited differentiation into proliferative chondrocytes indicated that DR enhanced the proliferation of resting chondrocytes while reducing the proliferation of more differentiated proliferative chondrocytes. To test this observation, we examined the incorporation of EdU into the growth plate to assess the proliferation of proliferative chondrocytes. When EdU was administered 2 h before euthanasia, the DR mice exhibited fewer EdU$^+$ cells in the growth plate than the control mice (10.0% ± 2.9% versus 0.9% ± 0.5%; Fig. 3l–n). Because there was little EdU uptake into resting chondrocytes, we performed in situ hybridization of *Ki67* and immunostaining for phospho histone H3 (p-H3) to assess the proliferation of resting chondrocytes. The results showed that the DR mice had a higher percentage of *Ki67$^+$* cells among ZsGreen$^+$ resting chondrocytes (40.8% ± 11.1% versus 55.8% ± 9.9%; Fig. 3o–q) and a higher percentage of p-H3-positive cells among ZsGreen$^+$ resting chondrocytes (12.6% ± 6.9% versus 26.8% ± 12.0%; Fig. 3r–t), suggesting that resting chondrocytes may increase mitotic activity during DR. Both the decrease in the number of resting chondrocytes exiting to the proliferative zone and the increase in the number of resting chondrocytes suggest that DR alters the balance between the self-expansion and differentiation of chondroprogenitor cells.

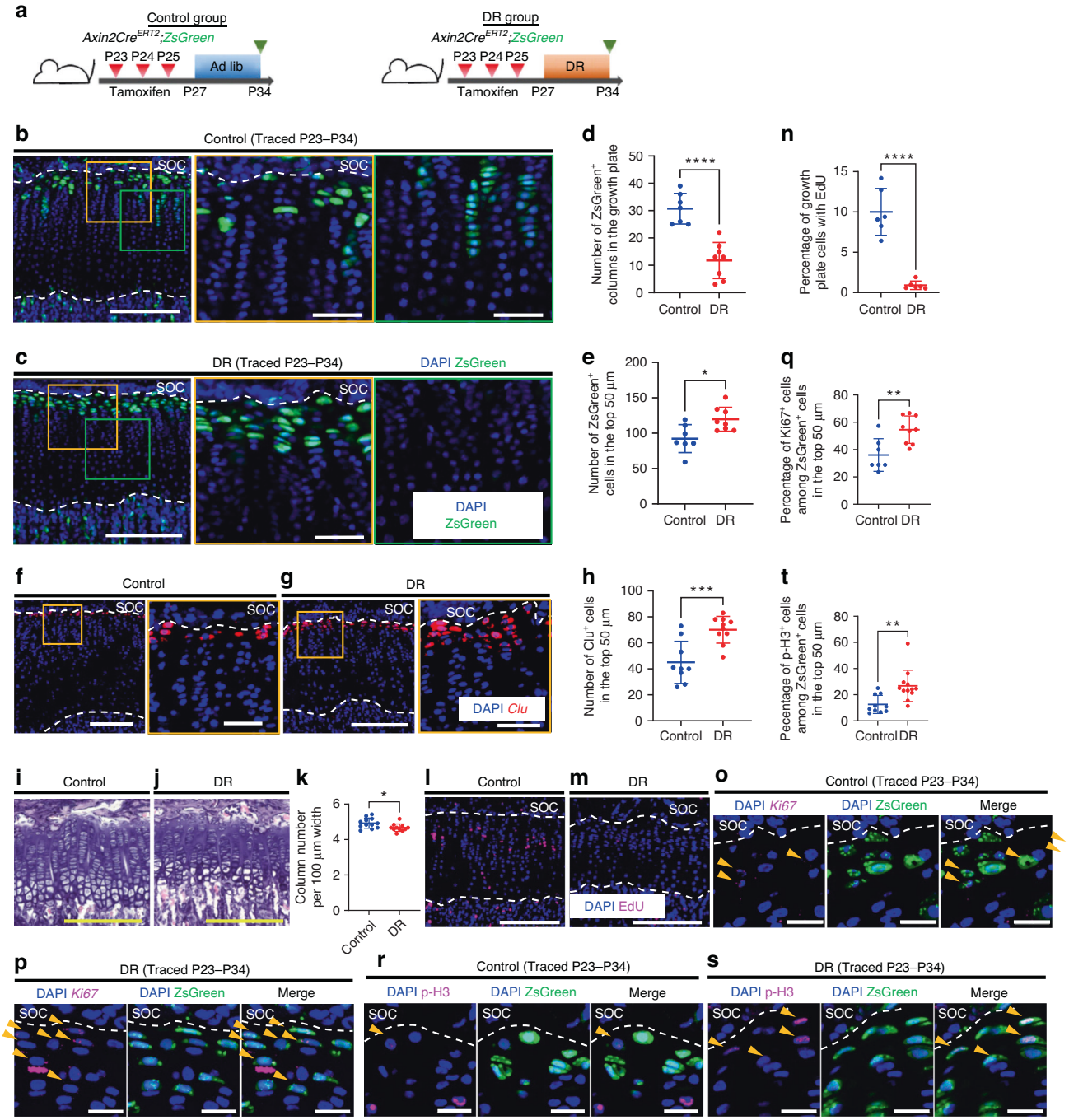

Fig. 3 Dietary restriction enhances the self-replication of resting chondrocytes while inhibiting their differentiation. **a** Schematic diagrams of the fate-mapping analysis of Axin2^{+} cells in the proximal tibial growth plate in *Axin2Cre^{ERT2};R26R^{ZsGreen}* mice (pulsed on P23–25 and traced for 11 days). **b**, **c** Representative images of descendants of initially labeled Axin2^{+} cells (ZsGreen^{+} cells) in the proximal tibial growth plate in the control (**b**) and DR (**c**) groups. **d**, **e** Quantification of the ZsGreen^{+} columns in the growth plate (**d**) and ZsGreen^{+} cells in the top 50 μm (**e**). Control group ($n = 7$), DR group ($n = 9$). $^{****}P =< 0.000\,1$ (**d**), $^{*}P = 0.012\,5$ (**e**). **f**, **g** Representative images for in situ hybridization of *Clu* in the proximal tibial growth plate in the control (**f**) and DR (**g**) groups. **h** Quantification of *Clu*$^{+}$ cells in the top 50 μm. Control group ($n = 9$), DR group ($n = 10$). $^{***}P = 0.000\,8$. **i**, **j** Representative images of hematoxylin and eosin staining of the proximal tibial growth plate in the control (**i**) and DR (**j**) groups. **k** Quantification of column number per 100 μm width of the growth plate. Control group ($n = 12$), DR group ($n = 11$). $^{*}P = 0.024\,5$. **l**, **m** Representative images of EdU labeling in the proximal tibial growth plate in the control (**l**) and DR (**m**) groups. EdU (50 μg·g^{-1} body weight) was injected two hours before euthanasia. **n** Percentage of growth plate cells with EdU. Control group ($n = 6$), DR group ($n = 6$). $^{****}P =< 0.000\,1$. **o**, **p** Representative images for in situ hybridization of *Ki67* and ZsGreen^{+} cells in the proximal tibial growth plate in the control (**o**) and DR (**p**) groups. Arrow heads, ZsGreen^{+} cells expressing *Ki67* (**o**, **p**). **q** Percentage of *Ki67*$^{+}$ cells among ZsGreen^{+} cells in the top 50 μm. Control group ($n = 7$), DR group ($n = 9$). $^{**}P = 0.004\,5$. **r**, **s** Representative images of immunostaining for p-H3 and ZsGreen^{+} cells in the proximal tibial growth plate in the control (**r**) and DR (**s**) groups. Arrow heads, ZsGreen^{+} cells expressing p-H3 (**r**, **s**). **t** Percentage of p-H3-positive cells among ZsGreen^{+} cells in the top 50 μm. Control group ($n = 10$), DR group ($n = 12$). $^{**}P = 0.003\,5$. Ad lib ad libitum, DR dietary restriction, SOC secondary ossification center, p-H3 phospho histone H3. The white dashed lines demarcate the growth plate from the surrounding tissues. Scale bars: 200 μm (**b** [left-most], **c** [left-most], **f** [left], **g** [left], **i**, **j**, **l**, **m**), 50 μm (**b** [right two], **c** [right two], **f** [right], **g** [right]), 20 μm (**o**, **p**, **r**, **s**). All data are presented as the mean ± SD. Statistical significance was determined by unpaired two-tailed *t* test

Ad libitum feeding after DR promotes committed differentiation of resting chondrocytes

Next, we assessed the changes in the distribution of *Axin2-CreER*$^+$ cells during the catch-up growth phase after DR. We compared the number of ZsGreen$^+$ cells in the top 50 μm and the number of ZsGreen$^+$ columns in the mice that were fed ad libitum after 7 days of DR (catch-up group) with those in the mice under continued DR (DR group) (Fig. 4a). Two days after ending DR (P36), *Axin2-CreER*$^+$ cells constituted a greater number of chondrocyte columns in the catch-up group than in the DR group (Fig. 4b, c, f), suggesting that the resting chondrocytes restarted differentiation into proliferative chondrocytes within 2 days after DR cessation. There were no significant differences in the number of ZsGreen$^+$ chondrocytes in the top 50 μm between the groups at this time point (Fig. 4b, c, g). Seven days after DR cessation (P41), *Axin2-CreER*$^+$ cells in the catch-up group had formed a greater number of ZsGreen$^+$ columns than those formed at 2 days after DR cessation (P36) (Fig. 4c, e, f), whereas the number of ZsGreen$^+$ columns remained unchanged in the DR group (Fig. 4b, d, f). This finding suggested that the pooled resting chondrocytes caused by seven-day DR retained the capacity to form chondrocyte columns. Seven days of feeding after DR cessation led to a 17% decrease in the number of ZsGreen$^+$ cells in the top 50 μm compared with that in the DR group (Fig. 4d, e, g). These data indicated that ad libitum feeding after stopping DR promoted the committed differentiation of resting chondrocytes.

The distribution of *Axin2-CreER*$^+$ cells in the catch-up group was then compared with that in the ad libitum control group (Fig. 4h). *Axin2-CreER*$^+$ cells constituted a significantly higher number of ZsGreen$^+$ chondrocyte columns in the catch-up group 14 days after stopping DR (P48) than that in the control group (Fig. 4m, n, o). DR inhibited the differentiation of resting chondrocytes into proliferative chondrocytes as described above. To assess the response of the resting chondrocytes to refeeding, we examined how much ZsGreen+ columns were increased from P34, completion of the diet restriction, to P36-P48, 2-14 days after refeeding. The average of the increased ratio was significantly higher in the catch-up group at P41 and P48 than in the control group (Fig. 4p). The increased column formation observed in the catch-up group theoretically contributed to the accelerated growth observed at P41 and P48 in the catch-up growth model (Fig. S7f, g). There were no significant differences in the number of ZsGreen$^+$ cells in the top 50 μm between the groups at all time points examined, although this number tended to increase beginning two days after DR cessation (P36) ($P = 0.18$) (Fig. 4i–n, q). The percentage of short columns among total columns in the catch-up group was 25.8% higher than that in the control group (75.7% ± 16.2% versus 49.9% ± 13.2%, $P = 0.043$; Fig. 4i, j, r) two days after stopping DR (P36). Progressive composition changes from short to long columns occurred in the catch-up group during ad libitum feeding ($P = 0.012\,6$), reducing this increase to 3.8% (not significant) at 14 days after stopping DR (P48) (Fig. 4r). This finding indicated that the pool of resting chondrocytes formed during DR comprised a heterogeneous cell population that included both short- and long-term chondroprogenitors. Together, these data demonstrated that external nutrition played an important role in determining the fate of chondroprogenitor cells in the resting zone.

IGF1/PI3K is activated in the resting zone of the growth plate

To understand the molecular mechanism by which external nutritional status regulates the fate of chondroprogenitors, we first investigated signaling pathways that were specifically activated in resting or proliferative chondrocytes by performing transcriptome analysis using laser microdissection (LMD) and RNA sequencing (RNA-seq) (Fig. 5a). We microdissected resting chondrocytes labeled with red fluorochrome-labeled and unlabeled proliferative chondrocytes in P30 tibial and femoral growth plates (Fig. S10a–c). Unsupervised clustering analysis showed that resting and proliferative chondrocytes clustered independently (Fig. S10d), indicating that resting chondrocytes had a biologically unique pattern of transcriptomes from those of proliferative chondrocytes. Statistical analysis revealed that 1 442 genes were differentially expressed between the two groups (fold change > ± 2, FDR < 0.01), of which 899 and 543 genes were upregulated in resting chondrocytes and proliferative chondrocytes, respectively (Fig. S10e). Representative genes upregulated in resting chondrocytes included previously reported markers for resting chondrocytes, such as *Clu*,[20] *Gas1*, *Wif1*,[21] *Efemp1*, and *Sorl1*[22] (Fig. S10e). Representative genes downregulated in the resting chondrocytes included *Acan, Col2a1, Matn1 and Slc2a1* (Fig. S10e). Downregulation of these genes in resting chondrocytes was confirmed by in situ hybridization (Fig. S10f). The expression of the markers for prehypertrophic chondrocytes, such as *Ihh*,[23] *Mef2c*,[24] and *Pth1r*,[25] was upregulated in the proliferative chondrocytes (Fig. S10e), which is likely due to the contamination of the prehypertrophic chondrocytes during excision of the proliferative chondrocytes.

Pathway analysis of differentially expressed genes (DEGs) revealed significant enrichment of several Kyoto Encyclopedia of Genes and Genomes (KEGG) pathways. KEGG pathways related to metabolism were often downregulated in resting chondrocytes, including metabolic pathways (KEGG: 01100), fatty acid metabolism (KEGG:01212), glycolysis/gluconeogenesis (KEGG: 00010), biosynthesis of unsaturated fatty acids (KEGG:01040), and biosynthesis of amino acids (KEGG: 01230) (Fig. S10g). These data indicated that resting chondrocytes showed unique metabolic regulation compared to proliferative chondrocytes. Among the pathways upregulated in resting chondrocytes, we focused on the phosphatidylinositol-3-kinase (PI3K) signaling pathway (KEGG:04151) (Fig. 5b) because it is affected by nutrient availability[26] and is required for normal growth plate differentiation and endochondral bone growth.[27] To confirm whether PI3K signaling was activated in resting chondrocytes, we examined the localization of phosphorylation of the protein kinase Akt (p-Akt), a downstream target of the PI3K pathway.[28] Immunohistochemistry of p-Akt showed that it was localized specifically in the resting and hypertrophic zones of the growth plate (Fig. 5c). Examination of upstream regulators through Ingenuity Pathways Analysis revealed more activated insulin-like growth factor 1 (IGF-1) signaling in resting chondrocytes than in proliferative chondrocytes (Table S1). Because the PI3K pathway is known as the major signaling cascade downstream of IGF-1 in many cell types,[29–32] these bioinformatics data suggested that IGF-1/PI3K signaling was activated in resting chondrocytes. Accordingly, the RNA-seq data showed significantly increased expression of *Igf-1* in the resting chondrocytes compared with that in the proliferative chondrocytes (Fig. 5d). In situ hybridization also demonstrated that *Igf-1* mRNA was localized in the resting zone of the growth plate, as well as in the perichondrium (Fig. 5e), and that *Igf1r* mRNA was ubiquitously expressed in growth plate chondrocytes, including Axin2$^+$ cells, in the resting zone (Fig. S11, arrowheads). Administration of picropodophyllin, an IGF-1 receptor tyrosine kinase inhibitor, reduced the percentage of p-Akt$^+$ cells in the resting zone (Fig. 5f–h), suggesting that the activated PI3K pathway in the resting chondrocytes was at least partially dependent on IGF-1 signaling.

IGF-1/PI3K signaling in resting chondrocytes changes in sync with nutritional availability

Because both IGF-1 and PI3K signaling are affected by nutritional status,[26,33,34] we investigated possible changes in the activity of IGF-1/PI3K signaling during DR and catch-up growth. We compared the serum levels of IGF-1 and the percentage of *Igf-1*$^+$ and p-Akt$^+$ cells among ZsGreen$^+$ resting chondrocytes in the mice in the catch-up group, nine-day DR mice (DR group), and

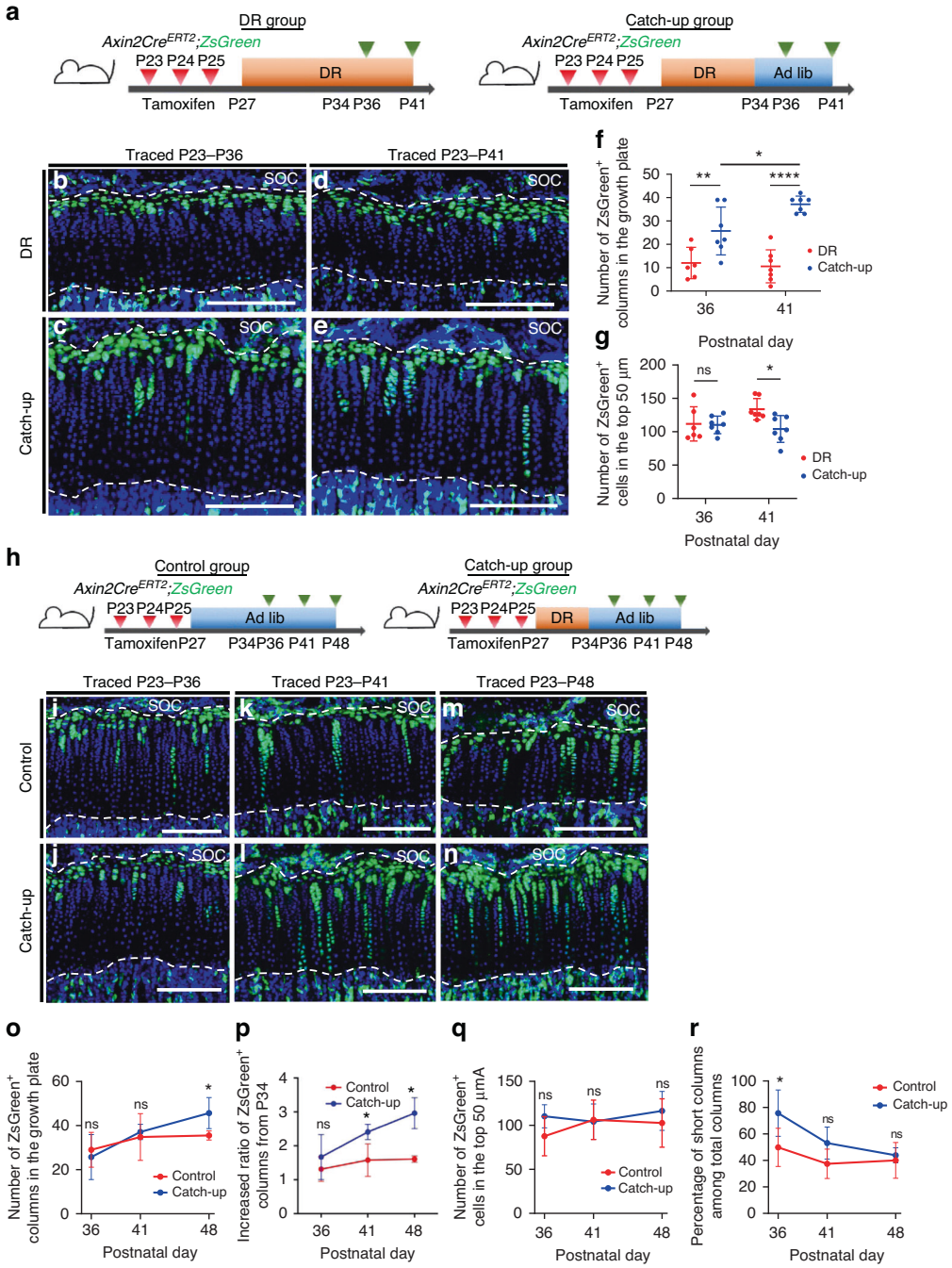

Fig. 4 Ad libitum feeding after dietary restriction promotes committed differentiation of resting chondrocytes. **a** Schematic diagrams of the fate-mapping analysis of Axin2^{+} cells in the proximal tibial growth plate in *Axin2Cre^{ERT2};R26R^{ZsGreen}* mice (pulsed on P23–25 and traced for 13 or 18 days). **b**–**e** Representative images of descendants of initially labeled Axin2^{+} cells (ZsGreen^{+} cells) in the proximal tibial growth plate in the DR (**b**, **d**) and catch-up (**c**, **e**) groups. **f**, **g** Quantification of the ZsGreen^{+} columns in the growth plate (**f**) and ZsGreen^{+} cells in the top 50 μm (**g**). DR group ($n = 6$), catch-up group ($n = 7$) at P36. DR group ($n = 7$), catch-up group ($n = 7$) at P41. Adjusted $^{*}P = 0.022$ (P36 vs. P41 in the catch-up group), adjusted $^{**}P = 0.005\,2$ (DR vs. catch-up, P36), adjusted $^{****}P = < 0.000\,1$ (DR vs. catch-up, P41) (**f**), adjusted $P > 0.999\,9$ (ns) (DR vs. catch-up, P36), adjusted $^{*}P = 0.015\,7$ (DR vs. catch-up, P41) (**g**). **h** Schematic of the fate-mapping analysis of Axin2^{+} cells in the proximal tibial growth plate in *Axin2Cre^{ERT2};R26R^{ZsGreen}* mice (pulsed on P23–25 and traced for 13, 18, or 25 days). **i**–**n** Representative image of ZsGreen^{+} cells in the proximal tibial growth plate in the control (**i**, **k**, **m**) and catch-up (**j**, **l**, **n**) groups. **o**–**r** Quantification of the number of ZsGreen^{+} columns in the growth plate (**o**), the increased ratio of the number of ZsGreen^{+} columns compared to the number at P34 when refeeding started (**p**), ZsGreen^{+} cells in the top 50 μm (**q**), and percentage of short columns among total columns (**r**). Control group ($n = 7$), catch-up group ($n = 7$) at P36 and P41. Control group ($n = 6$), catch-up group ($n = 6$) at P48. Adjusted $P > 0.999\,9$ (ns) (P36), adjusted $P > 0.999\,9$ (ns) (P41), adjusted $^{*}P = 0.046\,1$ (P48) (**o**). Adjusted $P = 0.374\,3$ (ns) (P36), adjusted $^{**}P = 0.004\,3$ (P41), adjusted $^{****}P = < 0.000\,1$ (**p**). Adjusted $P = 0.186\,5$ (ns) (P36), adjusted $P > 0.999\,9$ (ns) (P41, P48) (**q**). Adjusted $^{*}P = 0.042\,9$ (P36), adjusted $P = 0.100\,3$ (ns) (P41), adjusted $P > 0.999\,9$ (ns) (P48) (**r**). Ad lib ad libitum, DR dietary restriction, ns not significant, SOC secondary ossification center. The white dashed lines demarcate the growth plate from the surrounding tissues. Scale bars: 200 μm (**b**–**e** and **i**–**n**). All data are presented as the mean ± SD. Statistical significance was determined by two-way analysis of variance and Bonferroni's multiple comparison test

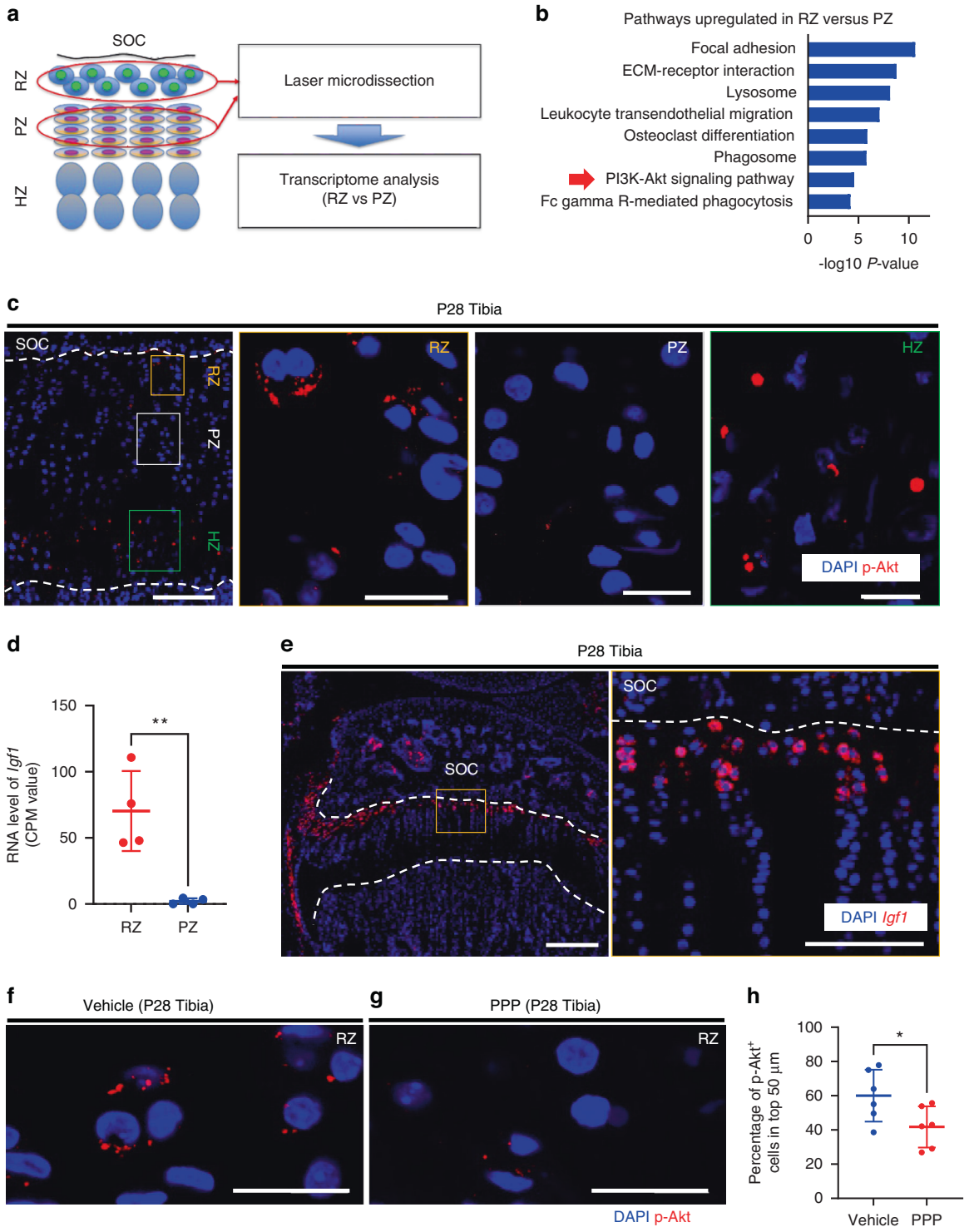

Fig. 5 IGF-1/PI3K signaling is activated in the resting zone. **a** Schematic diagram for transcriptome analysis using laser microdissection and RNA sequencing. P30 tibial and femoral growth plates in *Axin2Cre*^{ERT2};*R26R*^{TdTomato} mice (pulsed on P23–25) were subjected to laser microdissection. **b** KEGG pathways enriched by genes significantly upregulated in the resting zone compared to the proliferative zone. The red arrow indicates the PI3-Akt signaling pathway. Logarithmic *P* values of significance are indicated on the *x*-axis. **c** Representative image of immunohistochemistry for p-Akt in the proximal tibial growth plate at P28. The right three panels show magnified views of each zone of the growth plate. **d** CPM values of *Igf-1* in the resting and proliferative zone samples. RZ ($n = 4$), PZ ($n = 4$). $^{**}P = 0.004\,1$. **e** Representative image for in situ hybridization of *Igf-1* in the proximal tibial growth plate at P28. The right panel shows a magnified view of the resting zone of the growth plate. **f**, **g** Representative image of immunohistochemistry for p-Akt in the resting zone of the proximal-tibial growth plate at P28 after receiving either vehicle (dimethyl sulfoxide/corn oil, 9:1) (**f**) or IGF-1 receptor tyrosine kinase inhibitor (PPP, 20 µg·g^{-1} body weight) (**g**) 30 min before euthanasia. **h** Percentage of p-Akt^{+} cells in the top 50 µm. Vehicle group ($n = 6$), PPP group ($n = 6$). $^{*}P = 0.043\,5$. p-AKT phosphorylation of the protein kinase Akt, SOC secondary ossification, RZ resting zone, PZ proliferative zone, HZ hypertrophic zone, CPM count per million, PPP picropodophyllin. The white dashed lines demarcate the growth plate from the surrounding tissues. Scale bars: 200 µm (**c** [left-most], **e** [left]), 100 µm (**e** [right]), 20 µm (**c** [right three], **f**, **g**). All data are presented as the mean ± SD. Statistical significance was determined by unpaired two-tailed *t* test

mice fed ad libitum (control group) (Fig. 6a). Serum IGF-1 levels were significantly reduced in the DR group compared to those of the control and were recovered to some extent in the catch-up group (Fig. 6b), suggesting that circulating IGF-1 levels changed depending on the nutritional status, as reported previously.[35] In situ hybridization revealed that local *Igf-1* expression was significantly reduced in the DR group compared to that of the control and was recovered to some extent in the catch-up group (Fig. 6c–f). The reduction in Igf1 expression in the DR group and its recovery in the catch-up group were confirmed at the protein level (Fig. S12). Similarly, the activity of PI3K signaling, as assessed by p-Akt expression, was significantly reduced by nine-day DR compared to that of the control group and recovered to control levels in the catch-up group (Fig. 6g–j). These data indicated that both endocrine and para/autocrine IGF-1 and PI3K signaling activity changed with nutritional status. To examine the causal relationship between reduced IGF-1 and PI3K signaling activity under DR, we tested whether rhIGF-1 administration reversed the reduction in PI3K signaling caused by nutritional deprivation. One day of fasting caused a significant decrease in the activity of PI3K signaling and decreased circulating IGF-1 and growth plate *Igf-1* levels compared to control values (Fig. 6k–p, r). Remarkably, this reduction in PI3K was ameliorated by administration of rhIGF-1 (Fig. 6q, r), suggesting the requirement of IGF-1 reduction for downregulation of PI3K signaling caused by nutrient deprivation.

Exogenous IGF-1 promotes committed differentiation of resting chondrocytes under DR

The finding that IGF-1 signaling in resting chondrocytes changed with nutritional availability indicated that external nutritional cues determined the fate of chondroprogenitors through IGF-1 signaling. To demonstrate that IGF-1 signaling mediates DR-dependent effects on chondroprogenitor cells, we examined whether exogenous IGF-1 could cancel the effect of DR on chondroprogenitor cells. DR mice received rhIGF-1 (1 $\mu g \cdot g^{-1}$ body weight) or a vehicle as a control for seven consecutive days during DR (Fig. 7a). There were no significant differences in body weight (data not shown), growth plate height, or hypertrophic zone height between the two groups (Fig. 7k, l). However, *Axin2-CreER*$^{+}$ cells generated more chondrocyte columns in the DR mice treated with rhIGF-1 than in the untreated DR mice (Fig. 7b–d), suggesting that inhibited differentiation of resting chondrocytes by DR was partially reversed by IGF-1 treatment. Similarly, histological findings showed that chondrocyte column density increased after rhIGF-1 treatment (Fig. 7i, j, m). Administration of rhIGF-1 led to a 17% reduction in the number of ZsGreen^{+} cells in the top 50 μm compared with that in the untreated DR mice (Fig. 7b, c, e). Accordingly, in situ hybridization of *Clu* showed that the number of *Clu*$^{+}$ resting chondrocytes was reduced by 26% after administration of rhIGF-1 (Fig. 7f–h). In situ hybridization of *Ki67* showed that administration of rhIGF-1 did not affect the percentage of *Ki67*$^{+}$ cells among ZsGreen^{+} resting chondrocytes (Fig. 7n–p). Together, these data demonstrated that the inhibitory effect of DR on the differentiation of resting chondrocytes was at least in part mediated by reduced IGF-1 signaling, and administration of exogenous IGF-1 enhanced the committed differentiation of resting chondrocytes without affecting their proliferation.

DISCUSSION

In this paper, we demonstrated the cellular dynamics of chondroprogenitors in response to external nutrition. We identified a specific cell population residing within a niche in the resting zone of the growth plate after SOC formation by analysis of the *Axin2Cre*^{ERT2}*;R26R*^{ZsGreen} mice. The Axin2^{+} cells included a subset of chondroprogenitors that self-renewed and contributed to growth plate maintenance by differentiating into proliferative chondrocytes. Under DR, these chondroprogenitors are pooled in the resting zone and inhibit their differentiation into proliferative chondrocytes. Once nutritional impairment improved, the pooled chondroprogenitors immediately resumed their differentiation and formed an accelerated rate of chondrocyte columns compared to the control, contributing to catch-up growth. In addition, we showed that nutritional deprivation reduced the activity of IGF-1 signaling in chondroprogenitors and changed the balance between the differentiation and self-expansion of chondroprogenitor cells (Fig. 7q).

Fate-mapping analyses using *Axin2Cre*^{ERT2} mice enabled us to directly visualize the dynamics of chondroprogenitors during DR and subsequent catch-up growth. The proliferation of chondroprogenitor cells in the resting zone has been proposed to be temporarily suppressed during malnutrition, thus preserving proliferative potential. Unused proliferative potential leads to catch-up growth after malnutrition improves.[10,36] Our results, however, suggest that under DR, chondroprogenitor cells entered the cell cycle without differentiating into proliferative chondrocytes, resulting in their accumulation. Given that these pooled chondroprogenitors immediately restarted differentiation after nutrition was reestablished, accumulation of this pool of chondroprogenitors may have prepared the growth plate for rapid growth once nutrients became available. In support of this hypothesis, DR has been shown to stimulate stem cell self-renewal across a wide array of tissue types, seen in intestinal,[37] hematopoietic,[38] hair follicle,[39] and neural[40] stem/progenitor cells. Our lineage tracing analyses using *Axin2Cre*^{ERT2} mice revealed a novel cellular mechanism of catch-up growth, suggesting that *Axin2Cre*^{ERT2} mice can be used to monitor the dynamics of chondroprogenitors under several growth inhibitory conditions or local injuries.

The present study showed that nutrient deprivation reduced the activity of both endocrine and para/autocrine IGF-1 signaling, leading to a change in chondroprogenitor behavior during DR. IGF-1 signaling is thought to be a candidate molecular mechanism involved in catch-up growth.[41] IGF-1 levels are increased in cases of human catch-up growth,[42] and IGF-1 signaling is necessary for catch-up growth in zebrafish in response to oxygen availability.[43] In addition, *Igf-1* knockout mice showed a specific growth plate phenotype with an expanded resting zone and a narrowed hypertrophic zone,[44] supporting our observations in this study. Previous studies further support the finding that IGF-1 signaling plays an important role in catch-up growth. The results showing that administration of rhIGF-1 did not rescue either the DR-induced growth plate and hypertrophic shortening (Fig. 7i–l) or the increased induction of chondroprogenitor cell cycle entry (Fig. 7n–p) suggest that IGF-1 signaling is not the only pathway involved in nutrient-induced catch-up growth. Other endocrine, paracrine and autocrine factors may regulate multiple cellular events in the growth plate, such as cell replication of the proliferative zone, hypertrophy and calcification in the hypertrophic zone, and the transition from cartilage to bone, in growth arrest and catch-up growth in response to nutritional changes. Further studies are needed to identify the specific signaling molecules that underlie catch-up growth.

Endocrine and para/autocrine IGF-1 signaling is a crucial regulator of growth plate function, as it promotes chondrocyte proliferation and hypertrophy.[45–47] However, the effects of IGF-1 signaling on resting chondrocytes, including whether they are targeted by IGF-1, remain largely unknown. In vitro studies using growth plate chondrocytes have yielded controversial results: some report that IGF-1 selectively acts on differentiated proliferative chondrocytes,[48] whereas others report that all types of growth plate chondrocytes respond to IGF-1 signaling.[49–51] In an in vivo study on hypophysectomized rats, Ohlson et al. [52] reported that IGF-1 administration did not affect the number of label-retaining cells (slow-cycling cells) in the resting zone, whereas growth hormone increased this number. In contrast, Hunziker

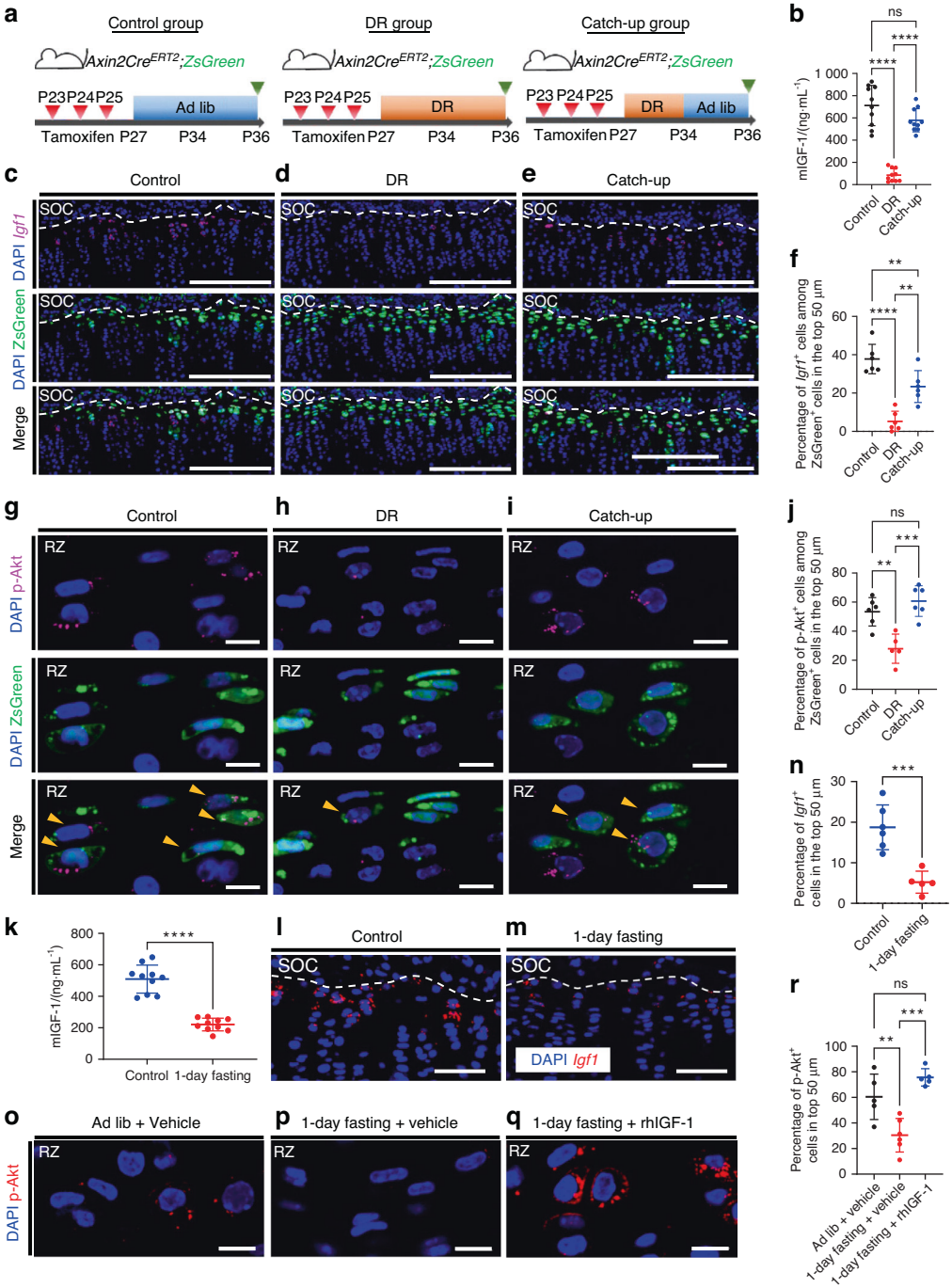

Fig. 6 IGF-1/PI3K signaling in resting chondrocytes changes in sync with nutritional availability. **a** Schematic diagrams of the fate-mapping analysis of Axin2^{+} cells in the proximal tibial growth plate in *Axin2Cre^{ERT2};R26R^{ZsGreen}* mice (pulsed on P23–25 and traced for 13 days). **b** Measurements of circulating IGF-1 levels in the sera from the control ($n = 10$), DR ($n = 10$), and catch-up ($n = 10$) groups. Adjusted ****$P < 0.000\,1$ (control vs. DR), adjusted ****$P < 0.000\,1$ (DR vs. catch-up), adjusted $P = 0.063\,1$ (ns) (control vs. catch-up). **c**–**e** Representative images of in situ hybridization of *Igf-1* and descendants of initially labeled Axin2^{+} cells (ZsGreen^{+} cells) in the proximal tibial growth plate in the control (**c**), DR (**d**), and catch-up (**e**) groups. **f** Percentage of *Igf-1*$^{+}$ cells among ZsGreen^{+} cells in the top 50 μm. Control group ($n = 6$), DR group ($n = 6$), catch-up group ($n = 6$). **g**–**i** Representative images of immunohistochemistry for p-Akt and ZsGreen^{+} cells in the resting zone of the proximal tibial growth plate in the control (**g**), DR (**h**), and catch-up (**i**) groups. **j** Percentage of p-Akt^{+} cells among ZsGreen^{+} cells in the top 50 μm. **k**–**n** Twenty-eight-day-old mice were fed ad libitum (control group) or subjected to one-day fasting (1-day fasting group). **k** Measurements of circulating IGF-1 levels in the sera of the control and one-day fasting groups. **l**, **m** Representative images for in situ hybridization of *Igf-1* in the proximal tibial growth plate in the control group ($n = 6$) (**l**) and the 1-day fasting group ($n = 5$) (**m**). **n** Percentage of *Igf-1*$^{+}$ cells in the top 50 μm. ***$P = 0.000\,8$. **o**–**r** Twenty-nine-day-old mice received vehicle (PBS) (vehicle group), vehicle followed by 1-day fasting (1-day fasting + vehicle group), or rhIGF-1 (1 μg·g^{-1} body weight) followed by 1-day fasting (1-day fasting + rhIGF-1 group). (**o**), 1-day fasting + vehicle group ($n = 6$) (**p**) and 1-day fasting + rhIGF-1 group ($n = 5$) (**q**). Percentage of p-Akt^{+} cells in the top 50 μm (**r**). Scale bars: 200 μm (**c**–**e**), 50 μm (**l**, **m**), 10 μm (**g**–**i**, **o**–**q**). All data are presented as the mean ± SD. Statistical significance was determined by one-way analysis of variance and Tukey's multiple comparison test (**b**, **f**, **j**, **r**) or by unpaired two-tailed *t* test (**k**, **n**)

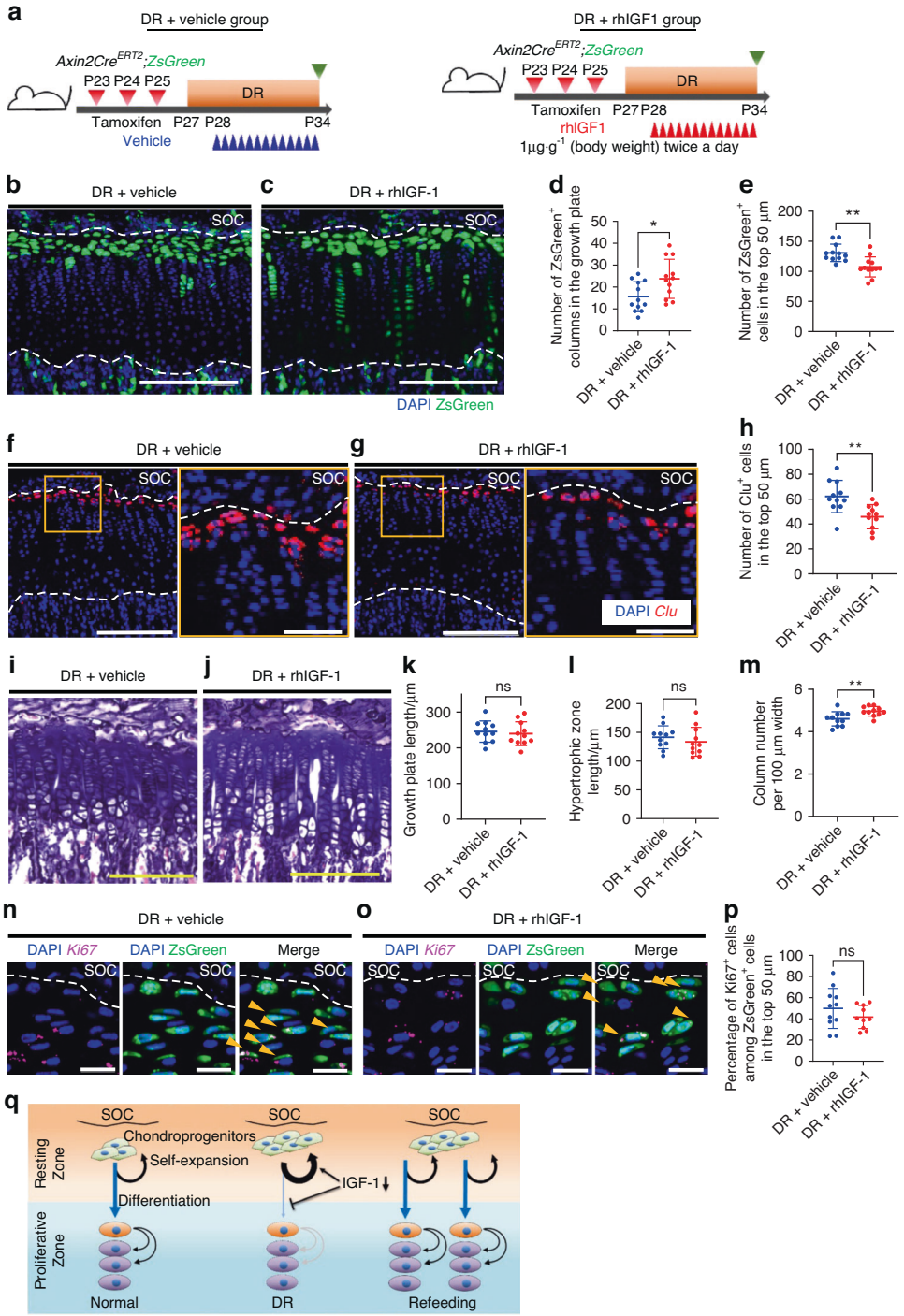

Fig. 7 Exogenous IGF-1 promotes committed differentiation of resting chondrocytes under dietary restriction. **a** Schematic diagrams of the fate-mapping analysis of Axin2^{+} cells in the proximal tibial growth plate in *Axin2Cre*^{ERT2};*R26R*^{ZsGreen} mice (pulsed on P23–25 and traced for 11 days). **b** Representative images of descendants of initially labeled Axin2^{+} cells (ZsGreen^{+} cells) in the proximal tibial growth plate in the DR + vehicle (**b**) and DR + rhIGF-1 (**c**) groups. **d**, **e** Quantification of the ZsGreen^{+} columns in the growth plate (**d**) and ZsGreen^{+} cells in the top 50 μm (**e**). DR + vehicle group ($n = 12$), DR + rhIGF-1 group ($n = 12$). **f**, **g** Representative images of in situ hybridization of *Clu* in the proximal tibial growth plate in the DR + vehicle (**f**) and DR + rhIGF-1 (**g**) groups. **h** Quantification of Clu^{+} cells in the top 50 μm. DR + vehicle group ($n = 11$), DR + rhIGF-1 group ($n = 11$). **i**, **j** Representative images of hematoxylin and eosin staining in the proximal tibial growth plate in the DR + vehicle (**i**) and DR + rhIGF-1 (**j**) groups. **k**–**m** Quantification of growth plate length (**k**), hypertrophic zone length (**l**) and column number per 100 μm width (**m**). $P = 0.666\,9$ (ns) (**k**), $P = 0.426\,4$ (ns) (**l**), $^{**}P = 0.008\,4$ (**m**). Data are presented as the mean ± SD. **n**, **o** Representative images for in situ hybridization of *Ki67* and ZsGreen^{+} cells in the proximal tibial growth plate in the DR + vehicle group (**n**) and the DR + rhIGF-1 group (**o**). Arrowheads, ZsGreen^{+} cells expressing *Ki67* (**n**, **o**). **p** Percentage of *Ki67*$^{+}$ cells among ZsGreen^{+} cells in the top 50 μm. **q** Graphical summary of how the dynamics of chondroprogenitors change during DR and refeeding. Scale bars: 200 μm (**b**, **c**, **f** [left], **g** [left], **i**, **j**, 50 μm **f** [right], **g** [right]), 20 μm (**n**, **o**). All data are presented as the mean ± SD. Statistical significance was determined by one-way analysis of variance and Tukey's multiple comparison test (**b**, **f**, **j**, **r**) or by unpaired two-tailed *t* test (**k**, **n**)

et al. [53] showed that exogenous IGF-1 application shortens the prolonged cell cycle time induced by hypophysectomy, demonstrating a stimulatory effect of IGF-1 on the mitosis of resting chondrocytes. Our findings suggest that IGF-1 signaling is activated in resting chondrocytes, changing with nutrient availability. Furthermore, exogenous IGF-1 promoted the committed differentiation of resting chondrocytes under restricted dietary conditions, indicating that IGF-1 acts on resting chondrocytes in vivo. In the present study, IGF-1 treatment reduced the number of resting chondrocytes (Fig. 7b, c, e) without changing their proliferative activity under DR conditions, as shown by *Ki67* expression (Fig. 7n–p). DR has been shown to increase the number of resting chondrocytes and allow their entry into the cell cycle, whereas hypophysectomy decreases the proliferative activity of resting chondrocytes.[53] The discrepancies between our data and previous in vivo studies are probably due to the different experimental conditions of IGF-1 administration (i.e., DR versus hypophysectomy). Further investigation is needed to elucidate the regulatory mechanisms of DR-induced enhancement of chondroprogenitor self-replication.

In summary, we elucidated the dynamics of chondroprogenitors and their regulatory mechanisms in response to nutrient availability. The current identification of these unique characteristics of chondroprogenitor cells in the growth plate has advanced our knowledge base of bone development and homeostasis. Furthermore, these findings may provide a means to develop noninvasive therapy for human growth disorders.

MATERIALS AND METHODS

Animals

All procedures were conducted according to the National Institutes of Health (NIH) guidelines and the Institutional Animal Care and USE Committee (IACUC) of the University of Maryland, Baltimore, protocol 0120006. *Axin2Cre^{ERT2}* (JAX018867), *Rosa26-CAG-loxP-stop-loxP-tdTomato* (Ai9:*R26R-tdTomato*, JAX007909), *Rosa26-CAG-loxP-stop-loxP-ZsGreen* (*Ai6:R26R-ZsG*, JAX007906), *Rosa26-CAG-loxP-stop-loxP-Confetti* (*R26R-Confetti*, JAX013731), and C57BL/6 J mice were obtained from the Jackson Laboratory. We crossed *Axin2Cre^{ERT2}* mice with *R26R-ZsG*, *R26R-tdTomato* or *R26R-Confetti* mice to create *Axin2Cre^{ERT2};R26R^{ZsGreen}*, *Axin2-Cre^{ERT2};R26R^{tdTomato}* or *Axin2Cre^{ERT2};R26R^{Confetti}* mice, respectively. For Cre recombination, 120 μg·g^{-1} (body weight) tamoxifen (T5648; Sigma–Aldrich) dissolved in corn oil (C8267; Sigma–Aldrich) was subcutaneously injected for three consecutive days from P0, P23, P42 or P84 in *Axin2Cre^{ERT2};R26R^{ZsGreen}* mice, for three consecutive days from P23 in *Axin2Cre^{ERT2};R26R^{tdTomato}* mice, and for five consecutive days from P23 in *Axin2Cre^{ERT2};R26R^{Confetti}* mice. All mice were housed in specific pathogen-free conditions and were allowed free access to food (Laboratory Autoclavable Rodent Diet 5010; LabDiet) and water, except during DR, as described later.

DR and catch-up growth

C57BL/6 J mice were used to establish a mouse catch-up growth model, and *Axin2Cre^{ERT2};R26R^{ZsGreen}* mice were used to perform lineage-tracing analyses. After six days of acclimatization in solitary cages, the mice were fed ad libitum or subjected to 50% of their normal food intake from P27 for the indicated periods. The normal intake was based on the intake of the C57BL/6 J mice fed ad libitum. During DR, food was provided once daily with ad libitum access to water. The mice were fed ad libitum after seven days of DR for catch-up growth.

Pharmacological modulation in vivo

For investigation of whether activation of PI3K signaling in resting chondrocytes is dependent on IGF-1 signaling, 28-day-old C57/B6J mice received intraperitoneal injections of either the IGF-1 receptor tyrosine kinase inhibitor picropodophyllin (PPP, 20 μg·g^{-1} body weight; SLK-S7668, Selleck Chemicals) or vehicle alone (dimethyl sulfoxide [D8418, Sigma–Aldrich]/corn oil, 9:1) 30 minutes before euthanasia.[54,55] For analysis of the relationship between IGF-1 and PI3K signaling under nutritional deprivation, 28-day-old C57/B6J mice were fasted for one day and then treated with a subcutaneous injection of either rhIGF-1 (1 μg·g^{-1} body weight; 291-G1, R&D Systems) or vehicle phosphate-buffered saline (PBS) alone 60 min before euthanasia. *Axin2Cre^{ERT2};R26R^{ZsGreen}* mice underwent catch-up growth treatment (see "DR and catch-up growth") and received subcutaneous rhIGF-1 (1 μg·g^{-1} body weight) or PBS twice daily (9:00 am and 18:00) for seven consecutive days from P28. Proximal tibias were collected 2 h after the final dose was administered at 9:00 on P34.

Measurement of tibial length

Radiographic lateral view images of the fixed tibia were taken using a Faxitron X-ray Specimen Radiography System (Hologic) in automatic exposure control mode. Images were analyzed using ImageJ software.

Histology and imaging

For hematoxylin and eosin staining, EdU staining, alizarin labeling, immunohistochemistry, and in situ hybridization, frozen sections at 5 μm were analyzed using Keyence BZX710 (Keyence) or Nikon CSU-W1 Spinning Disk Confocal Camera (Nikon). For lineage tracing analyses, frozen sections at 150 μm were analyzed using a Nikon CSU-W1 spinning disk confocal camera. Details are provided in the supplementary methods.

LMD and RNA-seq analysis

RNA was extracted from 8 μm snap frozen sections of distal femur and proximal tibial growth plates in *Axin2Cre^{ERT2};R26R^{TdTomato}* mice using the Picopure RNA Isolation Kit (KIT0204, Thermo Fisher) as previously described.[56] Microdissections of resting chondrocytes and proliferative chondrocytes were performed using a Leica LMD 7000 laser microdissection system (Leica Microsystems). RNA was amplified by two rounds of in vitro transcription using the Arcturus RiboAmp HS PLUS Kit (KIT0521, Thermo Fisher), and complimentary DNA libraries were prepared using the KAPA RNA HyperPrep Kit (Roche) according to the manufacturer's instructions. cDNA libraries were sequenced using an Illumina NovaSeq 6000 system. Raw and processed data are available in the Gene Expression Omnibus (GEO) database under accession number GSE192840. Details are provided in the supplemental methods.

Statistical analysis

Statistical analyses were performed using GraphPad Prism (version 6/9). All numerical results are presented as the mean ± SD from a minimum of three different experiments (the exact number is indicated in the figure legends). For single comparisons, data were tested for statistical significance using an unpaired two-tailed *t* test. For multiple comparisons, one-way analysis of variance (ANOVA) followed by Tukey's post hoc test was used. Comparisons between two groups and time points were performed using two-way ANOVA followed by Bonferroni's multiple comparisons. The *P* values of statistical significance are shown in the respective figures.

ACKNOWLEDGEMENTS

We thank L. Veronique (Children's Hospital of Philadelphia) and Q. Lin (University of Pennsylvania) for invaluable advice. We also thank K. Storm for professional editing of the manuscript. Research reported in this article was partially supported by the National Institute of Arthritis and Musculoskeletal and Skin Diseases of the National Institutes of Health under Award Number R01AR062908 (to MEI), R01AR056837 (to MI), R01AR073181 (to SO), and R21AR077654 (to SO), and the departmental fund of the University of Maryland (to MI, ME-I).

AUTHOR CONTRIBUTIONS

T.O. and M.E.I. devised the project, the main conceptual ideas and proof outline. T.O. performed a large part of the experiments. J.K., Y.U. and M.E.I. performed some experiments. K.W. and H.T. helped with the experiments. S.O. supported the microdissection and animal experiments. T.O., J.K. and M.E.I. analyzed the data, and Y.U., Y.O., T.S., S.T., M.I. and S.O. verified the data analysis. Y.I. performed bioinformatics analysis. T.O. and M.E.I. wrote the manuscript.

ADDITIONAL INFORMATION

Supplementary information The online version contains supplementary material available at https://doi.org/10.1038/s41413-023-00258-9.

Competing interests: M.I. is the spouse of M.E.I.

REFERENCES

1. Kronenberg, H. M. Developmental regulation of the growth plate. *Nature* **423**, 332–336 (2003).
2. Kember, N. F. Cell division in endochondral ossification. A study of cell proliferation in rat bones by the method of tritiated thymidine autoradiography. *J. Bone Joint Surg. Br.* **42B**, 824–839 (1960).
3. Abad, V. et al. The role of the resting zone in growth plate chondrogenesis. *Endocrinology* **143**, 1851–1857 (2002).
4. Mizuhashi, K. et al. Resting zone of the growth plate houses a unique class of skeletal stem cells. *Nature* **563**, 254–258 (2018).
5. Newton, P. T. et al. A radical switch in clonality reveals a stem cell niche in the epiphyseal growth plate. *Nature* **567**, 234–238 (2019).
6. Renthal, N. E., Nakka, P., Baronas, J. M., Kronenberg, H. M. & Hirschhorn, J. N. Genes with specificity for expression in the round cell layer of the growth plate are enriched in genomewide association study (GWAS) of human height. *J. Bone Miner. Res.* **36**, 2300–2308 (2021).
7. Black, R. E. et al. Maternal and child undernutrition: global and regional exposures and health consequences. *Lancet* **371**, 243–260 (2008).
8. Victora, C. G. et al. Maternal and child undernutrition: consequences for adult health and human capital. *Lancet* **371**, 340–357 (2008).
9. Prader, A., Tanner, J. M. & von, H. G. Catch-up growth following illness or starvation. An example of developmental canalization in man. *J. Pediatr.* **62**, 646–659 (1963).
10. Gafni, R. I. & Baron, J. Catch-up growth: possible mechanisms. *Pediatr. Nephrol.* **14**, 616–619 (2000).
11. Clevers, H., Loh, K. M. & Nusse, R. Stem cell signaling. An integral program for tissue renewal and regeneration: Wnt signaling and stem cell control. *Science* **346**, 1248012 (2014).
12. Lustig, B. et al. Negative feedback loop of Wnt signaling through upregulation of conductin/axin2 in colorectal and liver tumors. *Mol. Cell Biol.* **22**, 1184–1193 (2002).
13. van Amerongen, R., Bowman, A. N. & Nusse, R. Developmental stage and time dictate the fate of Wnt/beta-catenin-responsive stem cells in the mammary gland. *Cell Stem Cell* **11**, 387–400 (2012).
14. Lim, X. et al. Interfollicular epidermal stem cells self-renew via autocrine Wnt signaling. *Science* **342**, 1226–1230 (2013).
15. Wang, B., Zhao, L., Fish, M., Logan, C. Y. & Nusse, R. Self-renewing diploid Axin2(+) cells fuel homeostatic renewal of the liver. *Nature* **524**, 180–185 (2015).
16. Maruyama, T., Jeong, J., Sheu, T. J. & Hsu, W. Stem cells of the suture mesenchyme in craniofacial bone development, repair and regeneration. *Nat. Commun.* **7**, 10526 (2016).
17. Usami, Y. et al. Possible contribution of wnt-responsive chondroprogenitors to the postnatal murine growth plate. *J. Bone Miner. Res.* **34**, 964–974 (2019).
18. Chan, C. K. et al. Identification and specification of the mouse skeletal stem cell. *Cell* **160**, 285–298 (2015).
19. Murugan andan, S. et al. A FoxA2+ long-term stem cell population is necessary for growth plate cartilage regeneration after injury. *Nat. Commun.* **13**, 2515 (2022).
20. Haseeb, A. et al. SOX9 keeps growth plates and articular cartilage healthy by inhibiting chondrocyte dedifferentiation/osteoblastic redifferentiation. *Proc. Natl Acad. Sci. USA* **118**, e2019152118 (2021).
21. Hallett, S. A. et al. Chondrocytes in the resting zone of the growth plate are maintained in a Wnt-inhibitory environment. *Elife* **10**, e64513 (2021).
22. Lui, J. C. et al. Differential aging of growth plate cartilage underlies differences in bone length and thus helps determine skeletal proportions. *PLoS Biol.* **16**, e2005263 (2018).
23. St-Jacques, B., Hammerschmidt, M. & McMahon, A. P. Indian hedgehog signaling regulates proliferation and differentiation of chondrocytes and is essential for bone formation. *Genes Dev.* **13**, 2072–2086 (1999).
24. Arnold, M. A. et al. MEF2C transcription factor controls chondrocyte hypertrophy and bone development. *Dev. Cell* **12**, 377–389 (2007).
25. Hirai, T., Chagin, A. S., Kobayashi, T., Mackem, S. & Kronenberg, H. M. Parathyroid hormone/parathyroid hormone-related protein receptor signaling is required for maintenance of the growth plate in postnatal life. *Proc. Natl. Acad. Sci. USA* **108**, 191–196 (2011).
26. Xie, L. et al. Effects of dietary calorie restriction or exercise on the PI3K and Ras signaling pathways in the skin of mice. *J. Biol. Chem.* **282**, 28025–28035 (2007).
27. Peng, X. D. et al. Dwarfism, impaired skin development, skeletal muscle atrophy, delayed bone development, and impeded adipogenesis in mice lacking Akt1 and Akt2. *Genes Dev.* **17**, 1352–1365 (2003).
28. Brazil, D. P., Yang, Z. Z. & Hemmings, B. A. Advances in protein kinase B signalling: AKTion on multiple fronts. *Trends Biochem. Sci.* **29**, 233–242 (2004).
29. Galvan, V., Logvinova, A., Sperandio, S., Ichijo, H. & Bredesen, D. E. Type 1 insulin-like growth factor receptor (IGF-IR) signaling inhibits apoptosis signal-regulating kinase 1 ASK1*J. Biol. Chem.* **278**, 13325–13332 (2003).
30. McMullen, J. R. et al. Deletion of ribosomal S6 kinases does not attenuate pathological, physiological, or insulin-like growth factor 1 receptor-phosphoinositide 3-kinase-induced cardiac hypertrophy. *Mol. Cell Biol.* **24**, 6231–6240 (2004).
31. Radcliff, K. et al. Insulin-like growth factor-I regulates proliferation and osteoblastic differentiation of calcifying vascular cells via extracellular signal-regulated protein kinase and phosphatidylinositol 3-kinase pathways. *Circ. Res.* **96**, 398–400 (2005).
32. Kalluri, H. S., Vemuganti, R. & Dempsey, R. J. Mechanism of insulin-like growth factor I-mediated proliferation of adult neural progenitor cells: role of Akt. *Eur. J. Neurosci.* **25**, 1041–1048 (2007).
33. Underwood, L. E., Thissen, J. P., Lemozy, S., Ketelslegers, J. M. & Clemmons, D. R. Hormonal and nutritional regulation of IGF-I and its binding proteins. *Horm. Res.* **42**, 145–151 (1994).
34. Thissen, J. P., Ketelslegers, J. M. & Underwood, L. E. Nutritional regulation of the insulin-like growth factors. *Endocr. Rev.* **15**, 80–101 (1994).
35. Cheng, C. W. et al. Prolonged fasting reduces IGF-1/PKA to promote hematopoietic-stem-cell-based regeneration and reverse immunosuppression. *Cell Stem Cell* **14**, 810–823 (2014).
36. Baron, J. et al. Catch-up growth after glucocorticoid excess: a mechanism intrinsic to the growth plate. *Endocrinology* **135**, 1367–1371 (1994).
37. Yilmaz, O. H. et al. mTORC1 in the Paneth cell niche couples intestinal stem-cell function to calorie intake. *Nature* **486**, 490–495 (2012).
38. Chen, J., Astle, C. M. & Harrison, D. E. Hematopoietic senescence is postponed and hematopoietic stem cell function is enhanced by dietary restriction. *Exp. Hematol.* **31**, 1097–1103 (2003).
39. Forni, M. F. et al. Caloric restriction promotes structural and metabolic changes in the skin. *Cell Rep.* **20**, 2678–2692 (2017).
40. Lee, J., Seroogy, K. B. & Mattson, M. P. Dietary restriction enhances neurotrophin expression and neurogenesis in the hippocampus of adult mice. *J. Neurochem.* **80**, 539–547 (2002).
41. Rosello-Diez, A. & Joyner, A. L. Regulation of long bone growth in vertebrates; it is time to catch up. *Endocr. Rev.* **36**, 646–680 (2015).
42. Fattal-Valevski, A., Toledano-Alhadef, H., Golander, A., Leitner, Y. & Harel, S. Endocrine profile of children with intrauterine growth retardation. *J. Pediatr. Endocrinol. Metab.* **18**, 671–676 (2005).
43. Kamei, H. et al. Role of IGF signaling in catch-up growth and accelerated temporal development in zebrafish embryos in response to oxygen availability. *Development* **138**, 777–786 (2011).
44. Wang, J., Zhou, J. & Bondy, C. A. Igf1 promotes longitudinal bone growth by insulin-like actions augmenting chondrocyte hypertrophy. *Faseb J.* **13**, 1985–1990 (1999).
45. Wang, Y. et al. IGF-1R signaling in chondrocytes modulates growth plate development by interacting with the PTHrP/Ihh pathway. *J. Bone Miner. Res.* **26**, 1437–1446 (2011).
46. Cooper, K. L. et al. Multiple phases of chondrocyte enlargement underlie differences in skeletal proportions. *Nature* **495**, 375–378 (2013).
47. Lui, J. C., Nilsson, O. & Baron, J. Recent research on the growth plate: recent insights into the regulation of the growth plate. *J. Mol. Endocrinol.* **53**, T1–T9 (2014).
48. Lindahl, A., Nilsson, A. & Isaksson, O. G. Effects of growth hormone and insulin-like growth factor-I on colony formation of rabbit epiphyseal chondrocytes at different stages of maturation. *J. Endocrinol.* **115**, 263–271 (1987).
49. Hill, D. J. Stimulation of cartilage zones in the calf costochondral growth plate in vitro by growth hormone dependent plasma somatomedin activity. *J. Endocrinol.* **83**, 219 (1979).
50. Makower, A. M., Wroblewski, J. & Pawlowski, A. Effects of IGF-I, EGF, and FGF on proteoglycans synthesized by fractionated chondrocytes of rat rib growth plate. *Exp. Cell Res.* **179**, 498–506 (1988).
51. Makower, A. M., Skottner, A. & Wroblewski, J. Binding of insulin-like growth factor-I (IGF-I) to primary cultures of chondrocytes from rat rib growth cartilage. *Cell Biol. Int. Rep.* **13**, 655–665 (1989).

52. Ohlsson, C., Nilsson, A., Isaksson, O. & Lindahl, A. Growth hormone induces multiplication of the slowly cycling germinal cells of the rat tibial growth plate. *Proc. Natl. Acad. Sci. USA* **89**, 9826–9830 (1992).
53. Hunziker, E. B., Wagner, J. & Zapf, J. Differential effects of insulin-like growth factor I and growth hormone on developmental stages of rat growth plate chondrocytes in vivo. *J. Clin. Invest.* **93**, 1078–1086 (1994).
54. Caselli, A. et al. IGF-1-mediated osteoblastic niche expansion enhances long-term hematopoietic stem cell engraftment after murine bone marrow transplantation. *Stem Cells* **31**, 2193–2204 (2013).
55. Lui, J. C. et al. Cartilage-targeted IGF-1 treatment to promote longitudinal bone growth. *Mol. Ther.* **27**, 673–680 (2019).
56. Mori, Y., Chung, U. I., Tanaka, S. & Saito, T. Determination of differential gene expression profiles in superficial and deeper zones of mature rat articular cartilage using RNA sequencing of laser microdissected tissue specimens. *Biomed. Res.* **35**, 263–270 (2014).